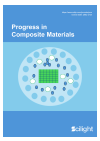
Scilight

Progress in Composite Materials
https://www.sciltp.com/journals/pcm



Article

Check for updates

Hierarchical Composites with Carbon Nanotube Grafted Carbon Fibers: A Critical Assessment

Mukul K. Srivastava [1], Himanshu Gupta [2], Nandini Gupta [2], Sumit Basu [1,*] and Prabhat K. Agnihotri [3]

[1] Department of Mechanical Engineering, Indian Institute of Technology Kanpur, Kanpur 208016, Uttar Pradesh, India
[2] Department of Electrical Engineering, Indian Institute of Technology Kanpur, Kanpur 208016, Uttar Pradesh, India
[3] Department of Mechanical Engineering, Indian Institute of Technology Ropar, Rupnagar 140001, Punjab, India
[*] Correspondence: sbasu@iitk.ac.in

How To Cite: Srivastava, M.K.; Gupta, H.; Gupta, N.; et al. Hierarchical Composites with Carbon Nanotube Grafted Carbon Fibers: A Critical Assessment. *Progress in Composite Materials* **2026**, *2*(1), 4. https://doi.org/10.53941/pcm.2026.100004

Received: 2 October 2026
Revised: 19 October 2026
Accepted: 22 October 2026
Published: 3 November 2026

Abstract: Carbon fiber reinforced polymer (CFRP) composites are engineered, synthetic materials of choice for an extensive range of applications, primarily in aerospace, automotive, wind turbine, and sports industries. Identifying viable technological pathways for increasing the range of properties that CFRPs currently offer might considerably widen the scope of their use. Hierarchical composites are made up of 'fuzzy fibers' or fibers that have been grafted with multiwalled carbon nanotubes. Apart from the important distinction that hierarchical composites use fuzzy fibers as reinforcement, they are similar to conventional CFRP composites in terms of manufacturing processes and resin system. Fuzzy fibers are synthesised through a variety of processes but the processing route involving high temperature chemical vapour deposition (CVD) is the most popular. We assess the possibility of using hierarchical composites synthesised via the CVD route as a replacement for conventional composites in situations that demand multi-functionality. This is motivated by the fact that improvements in Mode I and II fracture toughness and interlaminar shear strength without any loss of overall strength and stiffness is widely reported for hierarchical composites. Additionally, improvements in electrical properties, shielding to electromagnetic waves and thermal conductivity are also reported. We highlight the process-property relations in hierachical composites, attempt to identify the key process parameters and highlight the range of mechanical, thermal and electrical properties that have been obtained in our laboratory and by others. Finally, we attempt to identify area where hierarchical composites are most likely to find use as a versatile material.

Keywords: fuzzy carbon fiber; hierarchical composite; interlaminar fracture toughness; EMI shielding; thermal conductivity

1. Introduction

Since their demonstration on a laboratory-scale in the 1960s and the first large-scale commercial production in the 1970s, carbon fiber reinforced polymer (CFRP) composites have rapidly become the synthetic material of choice in a wide range of applications, with a current global demand exceeding 285 kilo-tonnes [1]. Not only has the aerospace industry adopted this highly engineered material with enthusiasm, non-aerospace applications have also emerged. Among these, CFRPs are in high demand as a material for wind turbine blades, and in the automotive, pressure vessel, sports leisure, and construction industries. These highly engineered materials typically have high specific strength, excellent corrosion resistance, and fatigue behavior. Convenient fabrication routes for large-scale production are now well-developed [2,3]. Given these reliable structural properties, the next challenge is to make them more versatile materials.

Is it possible to engineer more functionalities into CFRPs without compromising their existing properties and minimally modifying the established fabrication techniques? For example, can CFRP composites be used not only

Copyright: © 2026 by the authors. This is an open access article under the terms and conditions of the Creative Commons Attribution (CC BY) license (https://creativecommons.org/licenses/by/4.0/).
Publisher's Note: Scilight stays neutral with regard to jurisdictional claims in published maps and institutional affiliations.

as a reliable load-carrying member but also simultaneously store energy, provide shielding against external electromagnetic interference (EMI), resist weathering in outdoor applications and manage thermal loading during service conditions [4–9]?

A possible route to realising this goal involves replacing conventional carbon fibers with carbon fibers that have carbon nanotubes (CNTs) grafted on them. These fibers are called 'fuzzy carbon fibers' while the composites made with them are 'hierarchical CFRP composites'.

The first study on the feasibility of grafting carbon nanotubes (CNTs) on conventional carbon fibers seems to have been carried out by [10,11], based on the early work of [12,13]. fibers with grafted CNTs, also called 'fuzzy carbon fibers', were first used to make CFRP composites by [14]. Following their work, a number of studies have explored the possibility of using these hierarchical CFRP composites to meet the multifunctionality challenge.

This short paper is a critical assessment of the multifunctional properties of hierarchical composites based on our more than decade of experience with the fabrication and characterisation of these engineered materials. The paper is motivated by earlier work by others and us in establishing that optimisation of process parameters is the key to obtaining the best possible properties of hierarchical composites. Moreover, when the parameters are optimised adequately, hierarchical composites can potentially be excellent multifunctional materials. In particular,

1. we highlight the importance of processing parameters in determining various properties of these materials,
2. critically assess their expected advantages over conventional CFRP composites and
3. demonstrate that hierarchical composites are potentially attractive materials for some combinations of functionalities.

For a thorough review of the state of the art in hierarchical CFRP composites the reader is referred to [4].

Hierarchical CFRP composites provide some obvious advantages over other methods of incorporating CNTs in CFRP laminates. A competing strategy involves the addition of 1–3 vol% of CNTs in the polymer matrix and using this modified resin to prepare CFRP composites [15]. The CNTs are expected to create a very large volume fraction of interphase [16–18], which can potentially be engineered to increase the overall property of the composite [19]. However, this suffers from two well-known problems which limit the volume fraction of CNTs that can be added. Firstly, it is extremely difficult to ensure uniform dispersion of CNTs in polymer matrix beyond 1–3% volume fraction [20–23]. Secondly, the viscosity of the resin increases quite dramatically with the volume fraction of CNT. On the other hand, in hierarchical CFRP composites, grafting CNTs directly on the carbon fibers affects the fiber/matrix interface, which, in many situations, is the region where interfacial damage initiates.

In order to utilise the full technological potential of hierarchical composites and assess its benefits against conventional CFRP composites, in our view, two important issues must be addressed.

1. The process of synthesising fuzzy fibers or fabrics is crucial. Initial attempts at synthesising fuzzy fibers [24] reported significant loss of fiber strength due to the CVD process. Optimising the process parameters allows us to obtain fuzzy fibers that are almost as strong as conventional fibers. Also, as will be shown later, the length, density and the strength of the tethering point with the fiber can be controlled to a large extent by optimising process parameters. Most of these process parameters must lie within a narrow window for the best results. The first part of the paper focuses on the CVD process and optimum process parameters.
2. A critical comparison between physical properties obtained by various researchers becomes difficult because of different grades of epoxies, different types of carbon fibers, stacking sequences and test protocols used. In the second part of the paper, we compare results that are, as far as possible, limited to unidirectional (UD) laminates of hierarchical CFRP. Although differences in material grades still exist, comparison between results obtained on UD laminates help identify the most promising trends in hierarchical CFRP composites.

We have organised the paper as follows. In Section 2, the chemical vapour deposition (CVD) based synthesis protocol for grafted carbon fibers and woven fabrics is discussed. Properties of single grafted fibers are discussed in Section 3. In Section 4, we explore the gamut of physical properties that are affected by grafting. Finally, we discuss a few unexplored or unattained goals in Section 5.

2. Synthesising Grafted Carbon Fibers and Fabrics

Carbon nanotubes have been grown on single carbon fibers using many approaches such as electrophoresis, spray coating etc. [25–30]. But CVD based techniques seem to be the most promising because they offer scale-up possibilities, require limited equipment, and can potentially grow uniform CNT forests on complex surfaces [31,32] .

Carbon fibers grafted with CNTs (as discussed in the next section) form interfaces with polymers that have higher shear strength compared to as-received fibers. But, early attempts to graft CNTs in CVD-based processes led to grafted fibers with ∼30–50% lower tensile strength [24]. Subsequently, by carefully optimising the process parameters, grafted fibers with tensile strength and modulus comparable to as-received fibers have been

synthesised [24, 33]. This highlights the fact that mere grafting CNTs onto the fiber surface does not gurantee the improved composite properties. A through optimization of CVD growth parameters is needed to harness the excellent combination of CNTs properties in inducing multifunctionality to conventional CFRPs. It is to be noted here that the optimum parameters are a function of fiber specifications, type and resin chemistry. Typically, following steps are followed by an optimised CVD based process [34–39]:

1. The carbon fiber is preheated for ∼25 min in air at a temperature of 450 °C to remove the effect of any polymer sizing applied to it.
2. Electroless dip coating in an acidic bath containing Ni sulphate (as a source of Ni ions), sodium hypophosphite (as a reducing agent), sodium succinate (as a chelating agent) and succinic acid (to maintain a pH of ∼5–6) is used to coat Ni catalyst on the fiber surface. This is a crucial step in the grafting process to ensure uniform growth of CNTs on both sides of fiber fabric. The bath composition has been optimised in [40]. For instance, a coating time of 5 min at 75 °C with a bath composed of 30, 15, 15 and 0.36 g/L of Ni sulphate, sodium hypophosphite, sodium succinate and succinic acid respectively is reported to give good results [34].
3. The Ni catalyst-coated carbon fibers were put in a horizontal quartz tube reactor. Argon, hydrogen and acetylene were used as precursor gases.
4. At a temperature of 650 °C, the coated layer is reduced to Ni particles in a flowing hydrogen-nitrogen atmosphere.
5. Then, the temperature increases to 750 °C and a mixture of acetylene/argon (C_2H_2/N_2) at 40/100 sccm ratio is introduced into the reactor to grow the CNTs. The acetylene/argon flow is maintained for 5–25 min to obtain different lengths of CNTs and areal coverage of the fiber/fabric surface.
6. Finally, the furnace is cooled to room temperature in a Ar atmosphere.

A schematic of the CVD protocol described above is shown in Figure 1c. Furthermore, as shown in Figure 1a, the same CVD protocol can be used to graft CNTs on one or both sides of the received carbon fiber fabric layer depending on whether the catalyst coated fabric is placed in a quartz boat or suspended inside the CVD reactor [36]. When grown on a laminate, the optimised CVD protocol produces uniform coverage of individual fibers, as shown in Figure 2b.

The structure of the carbon fiber before and after CNT grafting is shown in Figure 2b. Note that typical diameter of a unsized carbon fiber is ∼7 µm. The diameter of grafted CNTs is in the range of 35–50 nm, while the length is a function of the C_2H_2/Ar flow time in the CVD. Raman spectra of grafted CNTs show characteristic peaks corresponding to D-band and G-band in CNTs in (see Figure 2a). The ratio of these peak intensities is ∼0.92, suggesting that the grafted CNTs are multi-walled and of moderate purity.

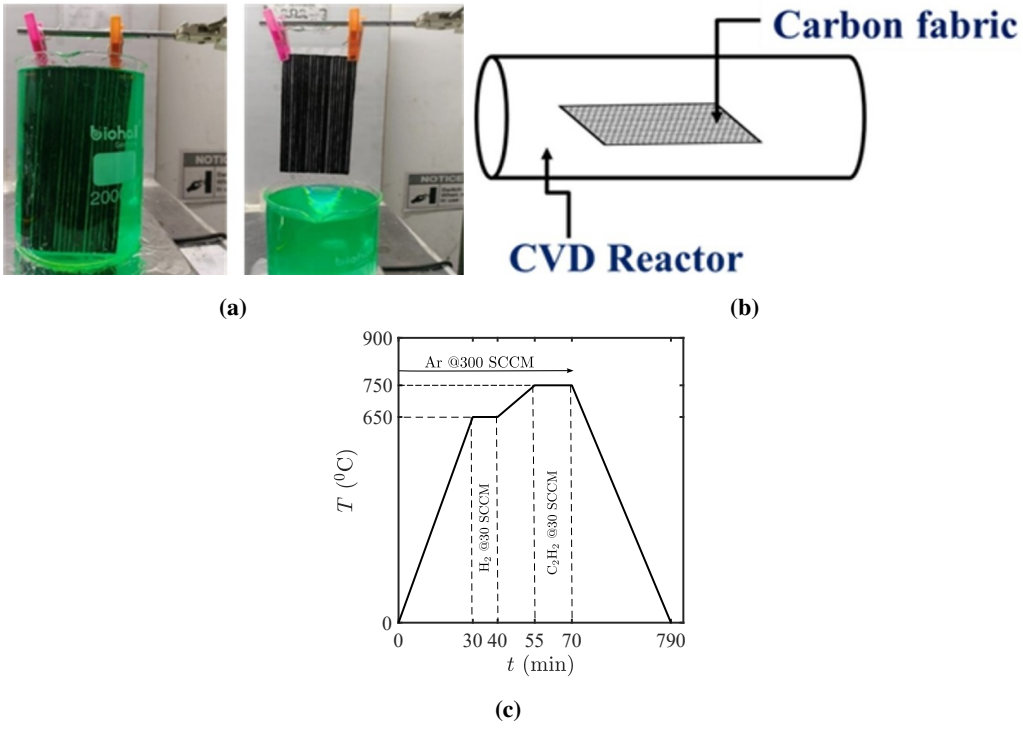
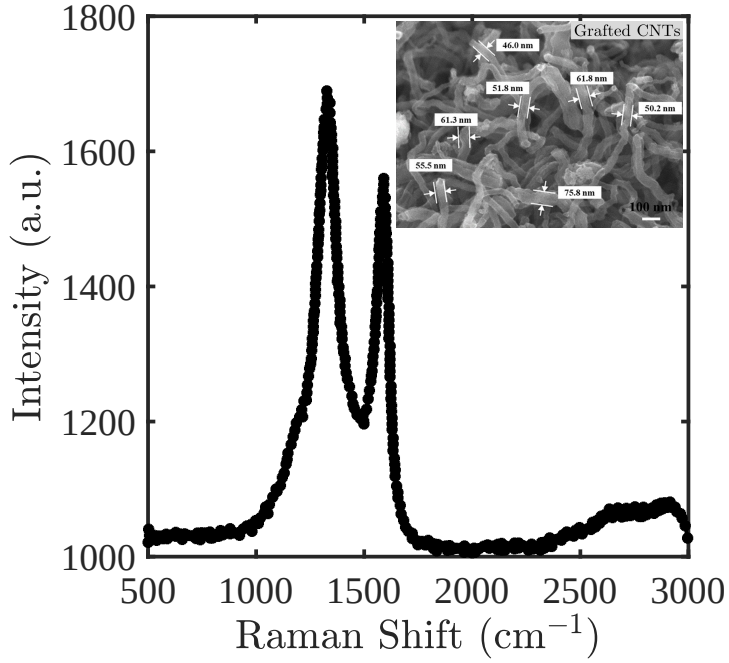
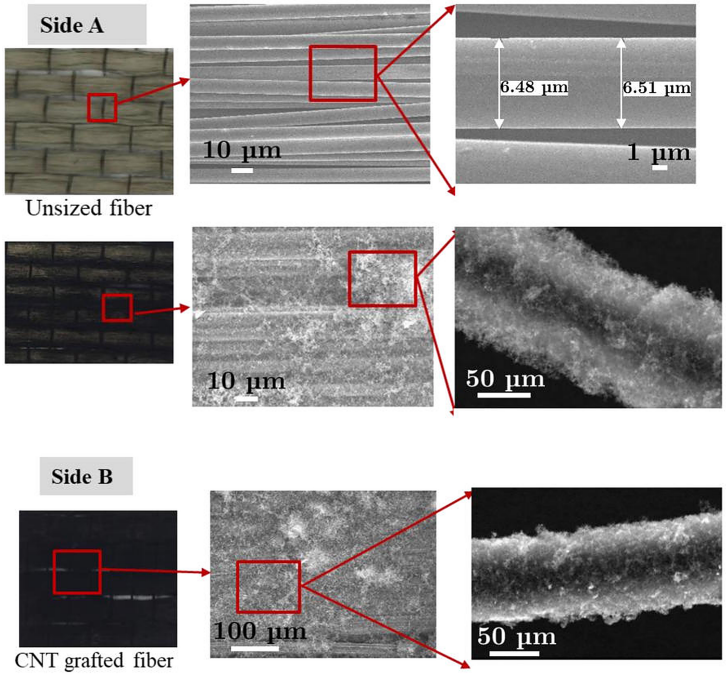


Figure 1. (**a**) Electroless dip coating bath for Ni catalyst coating on carbon fiber, (**b**) schematic of CVD reactor used for CNT grafting and (**c**) CVD protocol for CNT grafting on carbon fiber/fabric.



(a)



(b)

Figure 2. (**a**) SEM micrographs and Raman spectra of grafted CNTs and (**b**) optical and SEM micrographs of unsized and CNT grafted carbon fiber lamina showing uniform growth of CNTs on both sides of fiber fabric.

These CNT grafted fiber is then used to fabricate CNT modified CFRPs. CVD grafted CNTs show strong adhesion with the fiber surface [36–38] making it a preferred route to prepare CNT grafted fiber in comparison to other approaches such as electrophoresis, spray coating etc. [25–30].

3. Interfacial Mechanics of a Grafted Carbon Fiber

Carbon nanotubes grafted uniformly onto a carbon fiber create a finite size interphase region when embedded in a polymer matrix [33,38]. The variation of the elastic modulus along a radial line starting from the centre of the fiber cross-section can be mapped using careful nanoindentation studies [38]. These studies show that, while the interphase thickness depends on the length of the grafted CNTs (and hence on the growth time), it is comparable in magnitude to the fiber diameter. For instance, the thickness is ∼5 and ∼8 μm for growth times of 15 and 30 μm

respectively, compared to just 2 μm for an as-received fiber.

Careful design of the interphase region around each fiber is the key to increasing the interfacial shear strength (IFSS) of a grafted carbon fiber. The optimum growth conditions are therefore tailored to achieve the maximum IFSS. Pull-out [34,41] and fragmentation tests [5,42] are commonly used to measure the shear strength of a fiber matrix interface. The interfacial shear strength in turn, governs the strength and toughness of composite laminates made with the fiber fabric.

The interfacial shear strength of CNT grafted carbon fibers embedded in polymer matrices can be derived from pull out force versus pull out length plots obtained from single fiber pull-out tests [34]. The interfacial shear strength τ, improves strongly with CNT growth time to about 1.9 times that of the as-received fiber for a growth time of 20 min. However, for longer growth times, τ drops drastically. In other words, shear strength is maximum for a critical length of CNTs which is attained for a critical growth time t_{cr}. The non-monotonicity of the relation between shear strength and growth time is now well understood.

Computer models using the shear lag analysis and a specially designed cohesive zone model [34] for the interface leads to the following insights:

1. For growth time less than t_{cr}, both the length and surface coverage of CNTs is low. The polymer molecules and the CNTs provide strong anchoring of the fibers as shown in Figure 3a. The interface strength is limited by the fracture toughness of the polymer matrix. These interfaces are brittle and debond easily through the matrix.
2. In the post-debonded regime, the pull out force is governed by the coefficient of friction between the fiber and the matrix. The coefficient of friction between a debonded fiber and the polymer is higher when they are grafted. As a result, even after debonding, the fiber continues to support a substantial load in all cases.
3. For growth time greater than t_{cr}, the fibers are long and shear strength is limited by the strength of the tethering points. Debonding produces clean fibers which are then pulled out against friction (see Figure 3b).

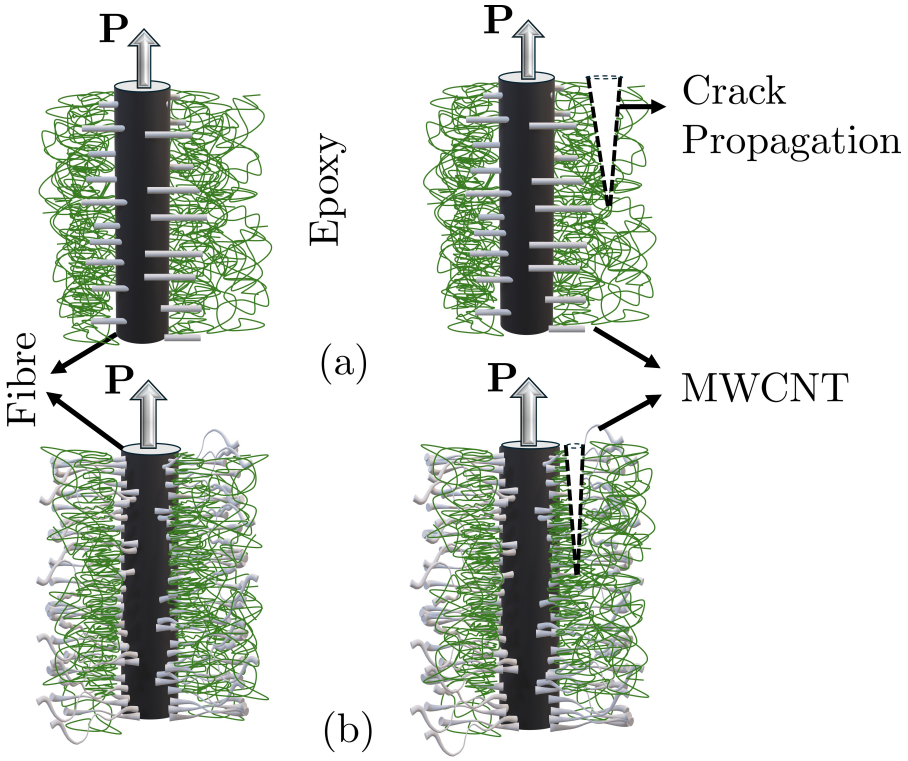


Figure 3. Possible failure mechanisms in pull out tests of CNT grafted carbon fiber in a polymer matrix corresponding to growth times (**a**) lower and (**b**) higher than t_{cr}.

So, to maximise the shear strength between the fiber and the matrix, synergy between two competing processes must be achieved. The CNTs must be grown to a length so that strong anchoring of polymer molecules can happen but failure from the tethering points does not. At the same time, they need to be grown densely so that the high friction between the CNTs and the polymer can be harnessed. The areal density of the CNTs depends directly on the size and spacing of the catalyst particles produced in Step 2 of the fabrication protocol in Section 2 [43]. In our CVD based grafting process, a growth time of 20 min (and the Ni coating process discussed in Section 2) achieves this

goal in the best possible way. Overall, a wider range of IFSS can be accessed by varying the CNT grafting process parameters. The relative improvement realized in composites depends on the interfacial microstructure [41,44–47].

Finally, as noted earlier, an optimised CVD process increases the IFSS by 1.5–1.9 times over as-received carbon fibers. Grafting of CNTs through other methods such as chemical grafting report similar improvements. For example, IFSS of 107.5 MPa is reported by [48]. It should be noted here that the IFSS of conventional CFRPs depends on the interfacial chemistry between polymer resin and fiber fabric. Therefore, a scatter in IFSS of reference CFRP coupons from various studies is expected.

Also, IFSS measured through fragmentation test (rather than pull out tests) show a wider scatter. For instance, with CVD-grafted fibers, Ref. [42] obtained a shear strength of 16 MPa while [5], using the electrophoretic route, has reported 70 MPa for similar systems.

Now that we have established that IFSS of single fuzzy fibers increases significantly over as-received ones, we turn to the question of how these single fiber level improvements translate to enhancement of properties in hierarchical composite laminates.

4. Comparison in Properties between Conventional and Hierarchical CFRP Composites

In order to ascertain whether CFRP composites with CNT grafted carbon fibers as reinforcement offer genuine technological advantages over conventional ones, we will critically compare them against a range of physical properties.

Apart from the processing parameters, the relative change in properties of hierarchical composites depends on the fiber/matrix grades, type of fabric and orientation of layers. This makes a quantitative comparison between experiments difficult. As benchmark cases, we will primarily use results obtained in our own laboratory for the discussion that follows. But, wherever pertinent, results from other groups will also be presented to highlight well-established trends in property improvements.

Our results on the other hand, are always for laminates that have the following characteristics. All comparisons are with conventional CFRP laminates fabricated with as received carbon fiber fabrics.

1. They use PAN-based unidirectional (UD) carbon fiber fabrics with an average modulus of 100 GPa, density of 1.8 g/cc, and weight 230 GSM, procured from Hindustan Technical Fabrics India.
2. The matrix is aerospace-grade epoxy Epofine-556 (Bisphenol-A) cured with Fine hard-5200 (amine hardener) in the weight ratio of 100:24, purchased from Fine Finish Organics Private Limited India.
3. All the laminates are cured following the curing protocol suggested by the supplier at 0.01 MPa curing pressure. All plies in laminates are stacked at 0° with respect to the length of the test specimen using hand layup method.
4. The volume fraction of fibers obtained from burn tests is very close to 60% in all composite coupons.
5. For fracture toughness testing where a pre-crack is required, a mylar sheet of 10 μm thickness is inserted at the midplane of the laminates.
6. The testing details for all properties are given in Appendix A.
7. In all discussion that follows, CFRP composites are made with CNT grafted on the carbon fiber fabrics using the protocol described in Section 2 and with the optimised process parameters.

4.1. Mechanical and Fracture Properties

There is near-unanimous agreement that the mechanical and fracture properties of hierarchical composites, fabricated through a controlled CVD-based process (as the one described in Section 2), are generally comparable to, and in many cases significantly better than, those of conventional CFRP composites.

For our samples, both the modulus and tensile strength of hierarchical UD composites in the direction of the fibers are almost identical to conventional CFRP composites. The Young's modulus and tensile strength for hierarchical composites are 95 GPa and 1005 MPa respectively, while the corresponding numbers are 96 GPa and 978 MPa for conventional composites (see Figure 4). As shown in Table 1, others studies too report marginal changes in Young's modulus and tensile strength.

The results in Figure 4 demonstrate that loss of strength and stiffness of carbon fibers due to the CVD-based grafting process pointed out by earlier works [24] can be mitigated by careful optimisaton of process parameters. Conventional and hierarchical UD laminates, when loaded in the fiber direction, respond in almost identical manner.

In fact, Ref. [38] shows that uniaxial properties in directions perpendicular to the fiber direction actually increases significantly for hierarchical UD laminates. This leads to two important inferences:

1. Uniaxial response in the fiber direction is not affected by grafting. It is governed almost entirely by the strength of the as-received carbon fibers.
2. Grafting improves interfacial stiffness which plays a role in off-0° loading directions.

Indeed, fracture surfaces under 0° loading show clean fiber-matrix interfacial failure while for off-0° loading we often see traces of epoxy sticking to the failed surface (see Figure 13 in [38]).

Table 1. Comparison between values of Young's modulus and tensile strength of UD conventional and hierarchical composites.

Property	Value for Conventional CFRP Composites	Value for Hierarchical Composites	Ref
Young's modulus (GPa)	∼135	140	[49]
	96	95	Our work
Tensile strength (MPa)	2600	2500	[49]
	1000	1200	[5]
	978	1005	Our work

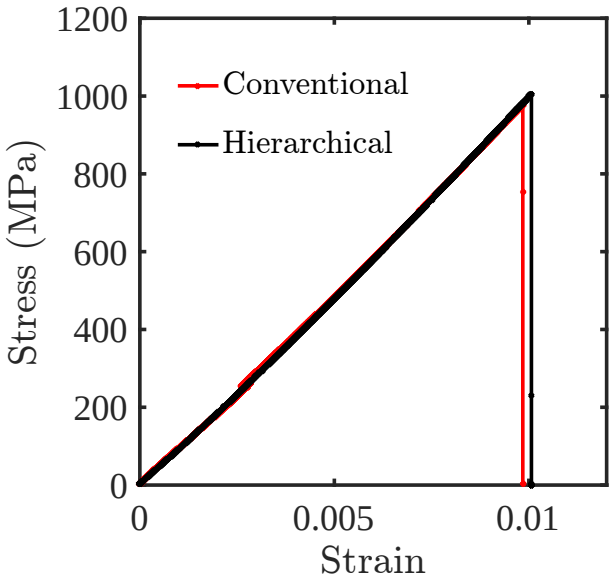


Figure 4. Uniaxial stress strain responses of UD laminates of hierarchical and conventional CFRP composites. Note the slight drop in Young's modulus and tensile strength for the hierarchical composite.

The strongest effect of using grafted carbon fibers is manifested in the increase in interlaminar shear strength (ILSS) and interlaminar fracture toughness, particularly in Mode II. This is a direct result of the increase in the shear strength of the fuzzy fiber-matrix interface [50] under optimal processing conditions.

The P-δ responses shown in Figure 5a, resistance curves in Figure 5b and $P_{\max}$ obtained from the P-δ response in Figure 5c are used to determine the ILSS, Mode I and Mode II interlaminar toughness respectively using the methods described in Appendix A.

For our samples ILSS increases from 45 MPa for conventional CFRP composites to almost 80 MPa for hierarchical ones. Similarly, Mode I interlaminar fracture toughness improves from 390 to 600 $\mathrm{J/m^2}$ (increase of 54%), and Mode II from 800 to 1500 $\mathrm{J/m^2}$ (increase of ∼87.5%) [36].

Increase in ILSS is most remarkable for fuzzy fibers produced through the CVD route. Other processing routes were much less successful in improving ILSS. Values of ILSS for conventional and hierarchical composites obtained by various authors are shown in Table 2. For example, in Ref. [51] sized carbon fibers with pre-functionalised CNTs were used but the improvement in ILSS was marginal. Similarly, Ref. [52] allowed CNTs to adsorb on the surface of unsized carbon fibers from an ultrasonicated aqueous solution. Again, the improvement in ILSS was marginal. On the other hand, all CVD based processes exhibit a near-doubling of the ILSS value.

A high ILSS alone does not indicate an improvement in interlaminar toughness. It is well-known that the short beam test does not produce a pure shear state in the specimen. As a result, it does not necessarily measure the energy required to propagate an interlaminar fracture. In fact, similar values of ILSS may be exhibited by specimens that undergo crushing, flexural or mixed failure rather than interlaminar debonding. So, we have also conducted dedicated fracture tests to ensure that the high ILSS measured for hierarchical composites is purely due to increase in interfacial toughness. The fact that Mode I and II interlaminar fracture toughness increases in tandem with ILSS proves that the increase in fiber-matrix shear strength is the cause of the enhancement.

Table 2. Comparison between values of ILSS of UD conventional and hierarchical composites.

Property	Value for Conventional CFRP Composites	Value for Hierarchical Composites	Ref
ILSS (MPa)	42.3	66.4	[53] (The as-received fibers were coated with polydopamine)
	62.7	77.7	[54]
	73.3	80.1	[51] (Carbon fibers were sized with pre-functionalised MWCNTs)
	23.0	50.0	[55]
	22.8	24.9	[52] (CNTs were adsorbed on fiber surface from an aqueous solution)
	45	80	Our work

Recent structural health monitoring (SHM) strategies [56] provide more direct evidence of the micromechanical failure processes during the ILSS test. Non woven silk fabrics decorated with CNT-MXene interspersed between conventional carbon fabric serve two purposes. They act as electrical resistance sensors and also increase the ILSS. The results in [56] show that the modified CFRP laminates record a sudden and large change in resistance when local damage initiates. The increase continues as cracks grow and proliferate. This allows identification of the global load at which damage initiates. Such SHM strategies are required to understand the exact sequence of events that lead to interlaminar failure in hierarchical composites.

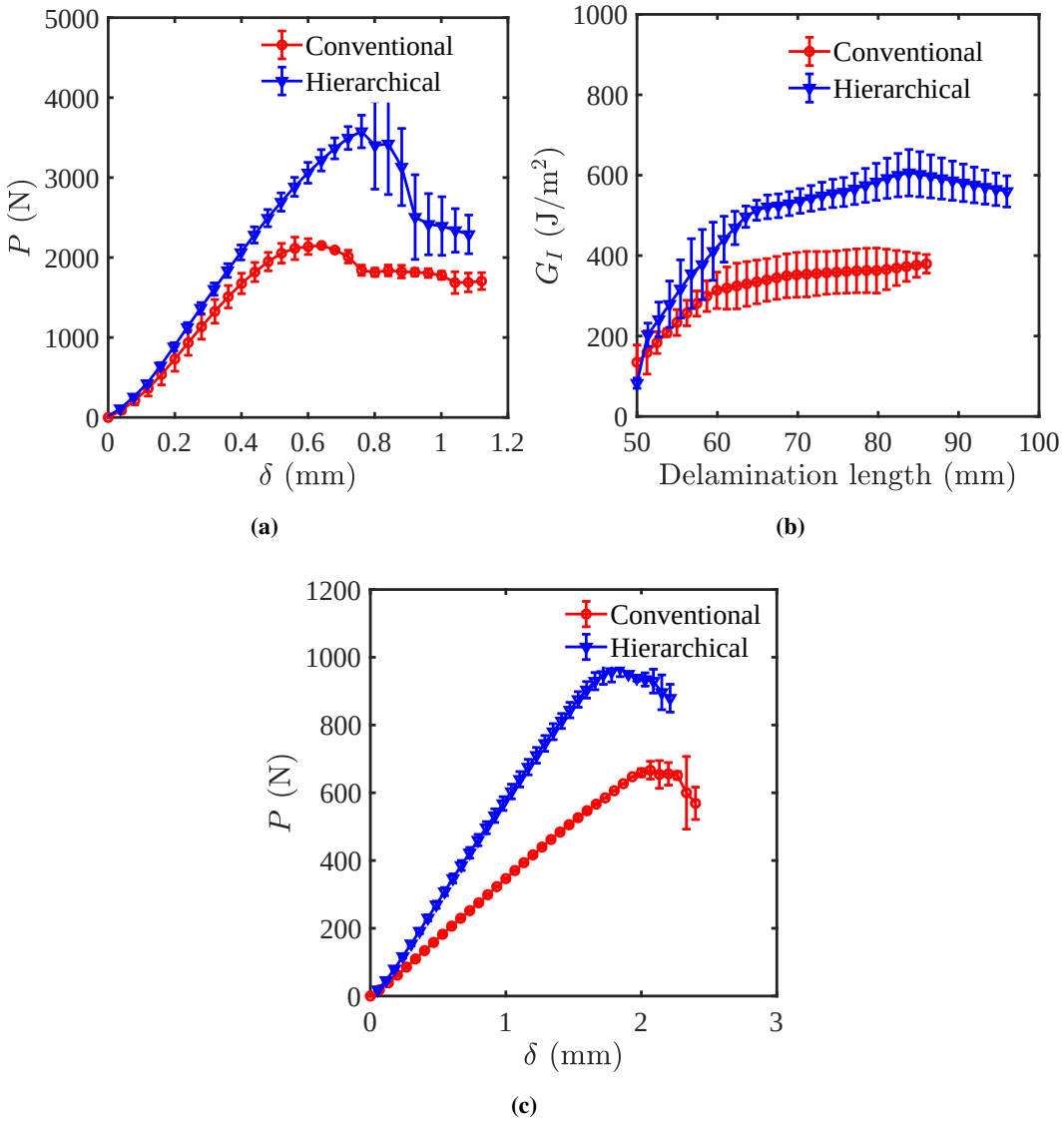


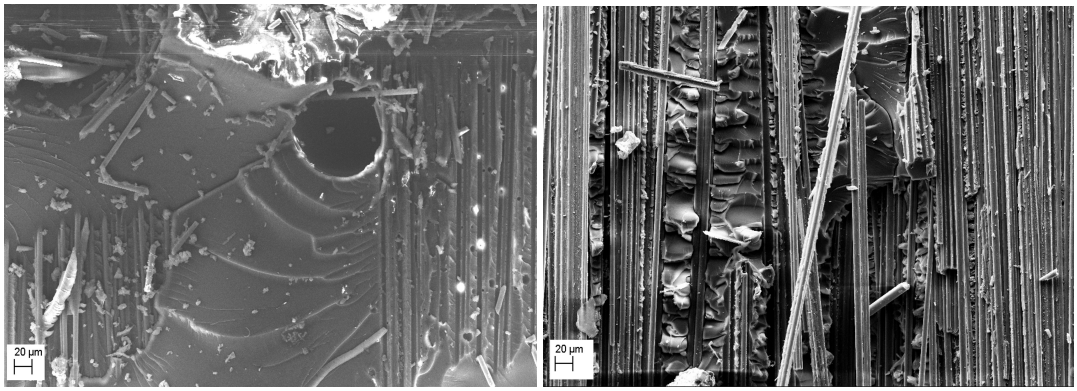
Figure 5. Force displacement (P-δ) curves for obtaining ILSS of conventional and hierarchical composites is shown in (**a**). The resistance curves for calculating G_{Ic} are shown in (**b**). The value of $P_{\max}$ in the P-δ curve is used for calculation G_{IIc} (**c**).

Increase in ILSS and interlaminar fracture toughness due to grafting is connected to the increase in IFSS under optimum synthesis conditions. Fracture surfaces for conventional and hierarchical laminates are compared in Figure 6. In both cases fracture surfaces are imaged at high resolution close to the pre-crack front under Mode I conditions. In the conventional composite, the fracture surface bears signatures of matrix cracking (note the river patterns on the epoxy matrix in Figure 6a) and clean fiber-matrix debonding. On the other hand, the hierarchical composite has a large number of broken fibers and signatures of textured microflow between fibers. The broken fibers indicate that due to the stronger fiber-matrix interface, fibers spanning the advancing crack continue to carry load behind the crack tip. They must subsequently debond, pull out, or break, which is potentially a much more energy-intensive process than either matrix cracking or fiber-matrix debonding.

The mechanism of strengthening in Mode II seems to be slightly different. Fracture surfaces of conventional and hierarchical composites under Mode II loading have been studied by [36]. In the case of conventional laminates, fractographs show clean fiber surfaces suggesting interfacial fracture. On the other hand, fracture surfaces in hierarchical composites show fibers with the matrix adhering to them. This indicates strong bonding between CNTs and fibers, due to which clean interfacial failure cannot occur.

Although there are fewer studies on the toughness of interfacial fractures, all existing ones corroborate the trends we observe. The review by [57] points out that the Mode I toughness depends more sensitively on the length of the grafted CNTs (and hence the growth time) than the Mode II toughness (see Figure 4 in [57]). Mode I toughness is unaffected for short growth times but upto 60% increase is seen when optimal growth times are used. The Mode II toughness, on the other hand, increases substantially even when sub-optimal growth times are used, and remarkably for optimal growth times.

Interestingly, very large increases in both Mode I and II fracture toughness are also obtained by using ingenuously fabricated interleaves. For example, Ref. [58] used interleaves of electrospun nylon nano-fibers decorated with –COOH– functionalised CNT surfaces. Interleaving, somewhat surprisingly, increases Mode I fracture toughness quite remarkably by 124%. Recall that CNT grafting of every ply in hierarchical composites leads to a much lower increase in Mode I toughness.



(a) **(b)**

Figure 6. Micrographs from scanning electron microscopy of Mode I fracture surfaces in (**a**) conventional and (**b**) hierarchical composites. The micrographs are from a region right next to the sharp pre-crack.

4.2. Electrical Properties

All studies agree that electrical conductivity of hierarchical composites is substantially higher than conventional ones. Single as-received carbon fibers have electrical conductivity of $\sim 2 \times 10^5$ S/m. In comparison, a CNT grafted single fiber prepared using the optimised CVD process parameters is 4 times more conductive [59].

Single fiber conductivity directly translates to conductivity of UD laminates. Expectedly, the increase in conductivity is the highest in the direction of the fibers. This increases from 400 S/m for conventional composites to 1000 S/m for hierarchical ones. In-plane transverse conductivity also increases from 4 to 20 S/m. Though the through thickness conductivity increases 6 times from 0.5 to 3 S/m, it is still low for many applications.

The electrical conductivity values reported by other researchers in cases where the CVD-based processing route was used, are presented in Table 3. Electrical conductivity, especially through the thickness, depends on the grafting process and the volume fraction of fibers. Particularly interesting are the very high values of in-plane conductivity reported by [60] and through thickness conductivity reported by [61]. In case of [60], the improvement is due to careful optimisation of the processing route. Also, the in-plane conductivity values reported are for woven fabrics rather than UD ones. The grafting in case of [61] was by a low temperature CVD process and the authors claim that

the CNTs in neighbouring plies touch each other to form a continuous electrical path through the thickness. High through-thickness conductivity is also reported by [6], where flame synthesised CNTs are grafted on carbon fabrics.

A direct consequence of the increased anisotropic conductivity is that laminates of hierarchical composites have improved shielding properties against electromagnetic waves. Computational studies of electromagnetic wave propagation through layered anisotropic media [62] have shown that rather than trying to increase the conductivity of the resin, a more feasible and effective strategy is to use more electrically conductive fibers. Fuzzy fibers with grafted CNTs being 4 times more conductive than as-received carbon fibers, are ideal candidates for enhancing shielding effectiveness.

The improvement is shielding effectiveness is almost entirely due to increase in absorbtion resulting from the increase in conductivity of the carbon fabric due to grafting. In both conventional and hierarchical composite laminate, reflection accounts for only 8–9 dB of the shielding effectiveness in the X-band [23,55].

Typically, shielding effectiveness is measured in two perpendicular orientations. The effectiveness is maximum when fibers of the UD laminates are aligned in the direction of the applied electric field while it is minimum when fibers are perpendicular to the electric field. In aerospace structures, shielding requirements are dictated by system-level standards such as RTCA DO-160 and MIL-STD-461. However, a baseline shielding effectiveness of 40–60 dB should be considered adequate for many aerospace applications.

In Figure 7, we compare the shielding effectiveness of conventional and hierarchical composites in the X-band, for both orientations. The shielding effectiveness is significantly higher for the hierarchical composite than for the conventional. Moreover, for both types of composites, shielding effectiveness is higher when the fibers are aligned along the electrical field (Figure 7a) than perpendicular to it (Figure 7b). In the X-band, the total shielding effectiveness increases from 40 to 50 dB in the direction of the fibers and from 20 to 30 dB in the transverse direction. A similar increase from 29 to 51 dB is reported by [55].

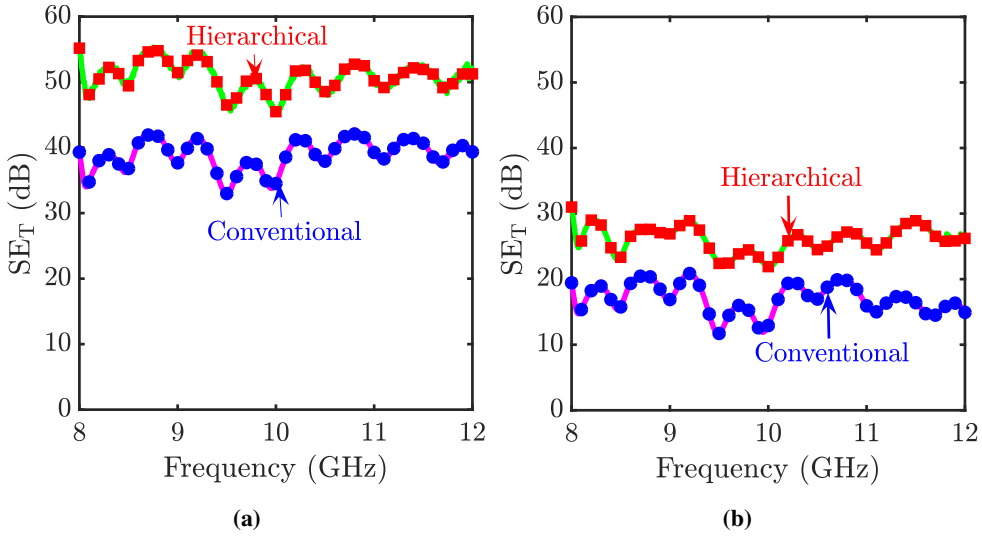


Figure 7. Total SE of conventional and hierarchical composite laminates with (**a**) carbon fibers aligned parallel and (**b**) transverse to the electric field.

Table 3. Comparison between values of in-plane and through thickness electrical conductivity of conventional and hierarchical composites.

Property	Value for Conventional CFRP Composites	Value for Hierarchical Composites	Ref
Electrical conductivity along the fiber (S/m)	138	149	[61]
	662	5882	[60]
	400	1000	Our work
Electrical conductivity across thickness (S/m)	23.7	38.4	[61]
	1.5	4	[55]
	4	20	Our work

4.3. Thermal Properties

Given the considerable increase in electrical conductivity, it is natural to expect that hierarchical composites will have higher thermal conductivity as well. The grafting of CNTs, which themselves have very high thermal conductivity, was expected to improve thermal transport. Unfortunately, this does not appear to be the case. The

anisotropic thermal conductivity of conventional and hierarchical composites is compared in Figure 8. The in-plane conductivity of both variants is high, especially in the direction of the fiber, where the values are comparable to the lower range of values obtained for metals. In fact, CNT grafting leads to considerable improvement in in-plane thermal conductivity.

However, the through-thickness thermal conductivity of hierarchical composites is marginally lower than conventional CFRP. The concentrated interphase in hierarchical composites, which play a major role in increasing toughness and ILSS, also offers very high thermal resistance. Consequently, CNT grafting does not have the desired effect on the through-thickness thermal conductivity. Molecular dynamics simulations on heat transport across the CNTs-epoxy interface [63] indicate that CNTs decorated with long functionalising molecules may be effective in reducing thermal resistance and increasing through-thickness conductivity.

We have used a custom designed set up to measure the in-plane conductivity, which is described in Appendix A. The through thickness conductivity is measured using a laser flash analyser [8]. Values of through-thickness conductivity reported by other researchers is listed in Table 3. While some studies show an increase in conductivity for hierarchical composites, the actual values are too low to be immediately useful in applications as heat sinks. Interestingly, the through-thickness thermal conductivity of carbon-carbon composites with carbon fiber fabric and pyrolitic carbon [64] is greatly benefited by CNT grafting on the fabrics (see Table 4). This again shows that the low conductivity of CFRP composites, both conventional and hierarchical, is due to the epoxy matrix.

The main reasons for the low through-thickness thermal conductivity of both conventional and hierarchical composites can be summarised as follows:

1. The epoxy-rich regions in both composites have very low thermal conductivity (0.2–0.25 W/mK).
2. There is very high thermal resistance at carbon-epoxy and CNT-epoxy interfaces.
3. The CNT-CNT contacts potentially have low thermal resistance but, for the reasons we discuss below, do not lead to sufficient improvement.

Grafting improves in-plane thermal conductivity in both along-fiber and transverse directions. The improvement in the along-fiber direction is due to the increase in conductivity of single fibers due to grafting. Further, when the process parameters are optimised properly, CNT forests grow almost radially outwards on the fiber surface. This means that CNT forests in neighbouring fibers overlap and create thermal bridges which, though not perfect, provide better transverse conductivity compared to conventional composites.

The fact that hierarchical composites show minimal increase in thermal conductivity but significant increase in electrical conductivity may seem counter-intuitive. The expectation that a material with high electrical conductivity will also possess high thermal conductivity arises from two considerations. Firstly, the correlation between thermal and electrical conductivity is established by the well-known Wiedemann–Franz law which is primarily for metals, where the mobile electrons carry both charge and heat. Secondly, individual CNTs posses extremely high thermal and electrical conductivities.

However, the mechanism of heat and charge conduction in hierarchical composites is very different from that in metals. In hierarchical composites, a CNT network is formed by CNT forests grown on neighbouring fibers and can provide a continuous percolating pathway for electrons. The establishment of a percolating CNT network can provide a sufficient number of CNT-CNT contacts that lead to significant reduction in electrical resistance. The situation is similar to that in pure epoxy-CNT nanocomposites [23].

On the other hand, heat in epoxy is transported primarily by phonons. When a phonon reaches the CNT–epoxy interface, large mismatch between the vibrational properties of the two materials results in a huge interfacial thermal resistance. Molecular dynamics (MD) simulations on epoxy-CNT interfaces [63] have demonstrated the effect of the interface thermal resistance. For instance, electrons can tunnel through a thin epoxy film between two highly conducting CNTs but the same film can effectively act as a barrier to heat transfer [23].

Table 4. Comparison between values of through thickness thermal conductivity of UD conventional and hierarchical composites.

Property	Value for Conventional CFRP Composites	Value for Hierarchical Composites	Ref
Through thickness thermal conductivity (W/mK)	0.61	0.94	[61]
	0.7	1.44	[6]
	8.11	38.74	[64]

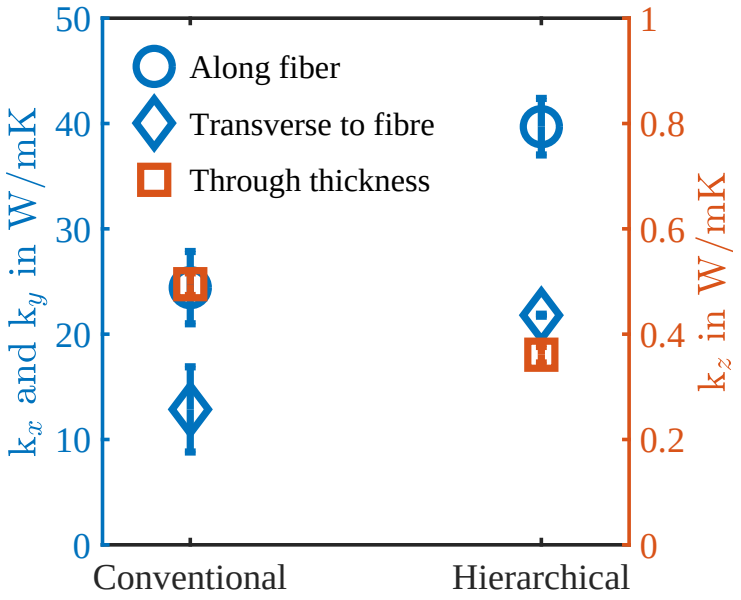


Figure 8. Values of anisotropic thermal conductivity conductivity for conventional and hierarchical composites are summarized. Here k_x, k_y and k_z are thermal conductivities along fiber, transverse to fiber and through thickness, respectively. Note that through-thickness thermal conductivity is measured using a laser flash analyser.

5. Outlook

A comparative summary of as-received and fuzzy carbon fibers is presented in Figure 9a. A similar comparative summary of hierarchical and conventional CFRP laminates is presented in Figure 9b. These figures give an overview of the demonstrated improvement achieved by grafting of CNTs.

Hierarchical CFRP composites using CNT-grafted carbon fibers exhibit mechanical properties equal to or better than conventional CFRP composites. Though the improvements, especially in ILSS and fracture toughness, are significant, they may not be enough to justify a large scale switch to hierarchical composites. A number of ongoing efforts may help in establishing hierarchical composites as a far more multi-functional and versatile replacement for conventional ones.

1. As the CVD-based processing technique for grafting CNTs on carbon fibers and fabrics is optimised on the laboratory scale, the next obvious step is to upscale it. Several continuous grafting processes have been proposed aimed at large scale production of carbon fibers with grafted [44,65] and vertically orientated [66] CNTs. In addition, processing routes with more precise control over spacing and distribution of grafted CNTs needs to be developed.
2. It has been demonstrated that hierarchical composites are potential multi-functional materials with excellent load-bearing capability. Areas where these materials can make potential impact are
   (a) As load bearing shields against electromagnetic radiation: As discussed in Section 4, shielding effectiveness between 40–50 dB has already been demonstrated for samples fabricated through the CVD route. Dry spraying of CNTs on carbon fiber fabrics have yielded even higher values of shielding effectiveness. Ref. [29] reports a minimum of 45 dB and maximum of 65 dB, which makes hierarchical composites a strong contender in strategic aerospace applications.
   (b) As structural batteries: Some recent studies [67,68] have explored the possibility of utilising hierarchical composites as load bearing energy storage materials, called ‘structural batteries’. Here the fuzzy carbon fibers serve as both reinforcements and electrodes. The primary challenge is in designing the matrix which must be stiff and, at the same time, function as an electrolyte. Two phase blends with epoxy and an organic liquid electrolyte are likely candidates for the matrix.
   (c) As the material of choice in load bearing outdoor applications: A somewhat under-explored property of hierarchical composites is their weather-resistance. In composites with as-received fibers but CNTs dispersed in the matrix, both Mode I and II interlaminar fracture toughness are retained after several hundred hours of accelerated weathering [35]. These results are expected to translate to hierarchical composites of the kind discussed here.

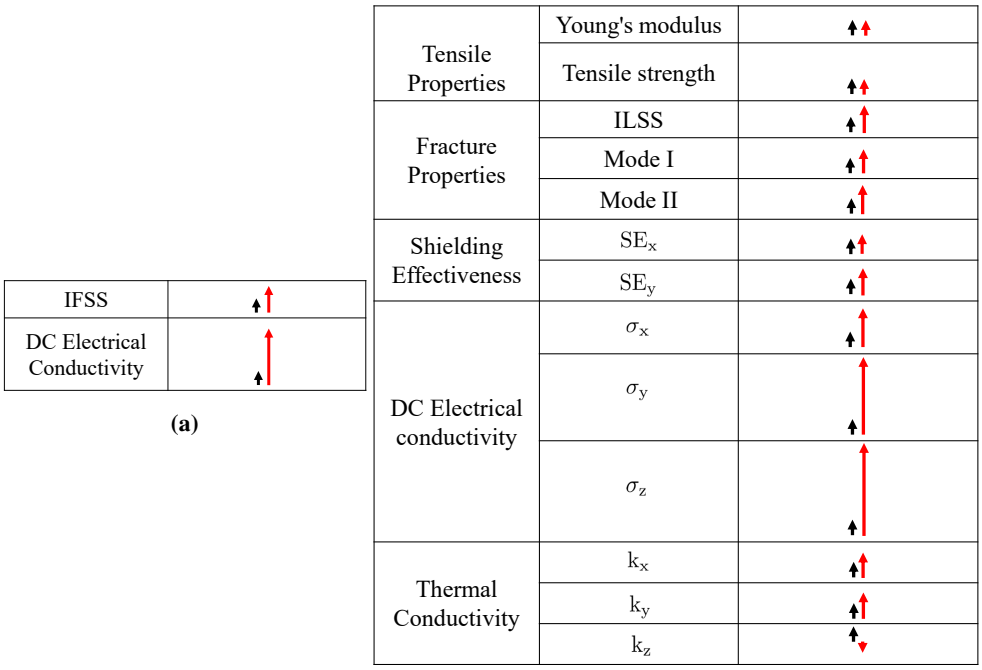


Figure 9. A comparative summary of the increase in various properties of (**a**) fuzzy fibers and (**b**) hierarchical composites (represented by red arrows) against as-received fibers and conventional CFRP composites (represented by red arrows) respectively. The relative sizes of the black and red arrows indicate the extent of increase. Downward arrows imply a decrease. For anisotropic properties, subscript x denotes the direction along fibers, y transverse to the fibers and z through the thickness.

Author Contributions

S.B.: Conceptualization, methodology, software; P.K.A., S.B., N.G.: Data curation, writing—original draft preparation; M.K.S., H.G.: Visualization, investigation; S.B., N.G.: Supervision; M.K.S.: Software, validation; S.B.: Writing—reviewing and editing. All authors have read and agreed to the published version of the manuscript.

Funding

The authors acknowledge the financial support received from ISRO (STC/ME/2019436) and DRDO (ARMREB/CDSW/2021/240) to carry out the research reported in this study.

Institutional Review Board Statement

Not applicable.

Informed Consent Statement

Not applicable.

Data Availability Statement

The data that support the findings of this study are available from the corresponding author upon reasonable request.

Acknowledgments

We would like to express our appreciation to Malkeet Singh for his assistance with the thermal conductivity experiments.

Conflicts of Interest

The authors declare no conflict of interest.

Use of AI and AI-Assisted Technologies

No AI tools were utilized for this paper.

Appendix A. Characterisation Techniques Used for Different Properties

Appendix A.1. Measuring the ILSS: Short Beam Test

The influence of CNTs grafting on the interlaminar shear strength (ILSS) of CFRPs is characterised by a 3-point short-beam shear test according to ASTM D2344 standard. The testing is performed on a universal testing machine (Zwick/Roell; Ulm, Germany) at a crosshead speed of 0.5 mm/min. The load-displacement data of the specimens are recorded and their respective ILSS is evaluated using the following relationship,

$$\tau = \frac{3P}{4bh} \tag{A1}$$

where τ is the apparent ILSS, P is the peak load, b and h are the width and thickness of the test specimen respectively.

Appendix A.2. Mode-I Fracture Toughness: Double Cantilever Beam (DCB) Test

The effect of CNT grafting on the Mode I fracture toughness of CFRPs is evaluated according to ASTM D5528 standard. The geometry and dimensions of the double cantilever beam (DCB) test coupons are taken according to the standard. Piano hinges are attached to the sample with Araldite adhesive (Pidilite Industries Limited, Basel, Switzerland). Cyclic tensile tests are performed in displacement control mode at a crosshead speed of 5 mm/min. Vertical grid lines are marked on the sample to record the crack extension in each cycle. Following the modified beam theory (MBT) data reduction scheme, the Mode I fracture toughness is calculated using the relation,

$$G_{Ic} = \frac{3P\delta}{2b(a+\Delta)}, \tag{A2}$$

where G_{IC}, P, δ, b, a and Δ are Mode I fracture toughness, peak load, load point displacement, specimen width, delamination length, and a correction factor that accounts for specimen rotation during the test.

Appendix A.3. Mode-II Fracture Toughness: End Notched Flexure Test

The effect of CNT grfting on the Mode II fracture toughness of CFRPs is evaluated following the ASTM D7905 standard. All the tests are performed in displacement control mode at a crosshead speed of 0.5 mm/min. The load-displacement data of the specimens are recorded. The modified beam theory data reduction scheme is used to evaluate the Mode II fracture toughness of the composite specimens using the following equation.

$$G_{IIc} = \frac{9P^2Ca^2}{2b(2L^3+3a^3)} \tag{A3}$$

where G_{IIC}, P, C, a, b, and L are Mode II fracture toughness, peak load, compliance, delamination length, specimen width, and half span length respectively.

Appendix A.4. Electrical Conductivity: Two Point Probe

Like thermal conductivity, electrical conductivity is also anisotropic. We use a Keithely-2460 SMU (Tektronix, Solon, Ohio, USA) with a two-point probe method to measure electrical conductivity. The electrical conductivity is examined along (σ_x), perpendicular to the fiber (σ_y), as well as through thickness (σ_z), as shown in Figure A1. The sample surfaces are polished before the measurement. Silver paste and a small clamping force are used to ensure effective contact between electrode probes and the sample. The sample dimensions are $30 \times 30 \times 2$ mm^3. Electrical conductivity is obtained using the following relation,

$$\sigma = \frac{L}{R_m A} = \frac{I_{\text{input}} L}{V_{\text{measured}} A} \tag{A4}$$

where σ is the electrical conductivity of the composite in the x, y, or z direction, I_{input} is the applied current, V_{measured} is the measured voltage, L is the distance between the electrodes, A is the cross-sectional area and R_m is the measured resistance. Average conductivity based on the multiple measurements for each sample is used for comparison purposes.

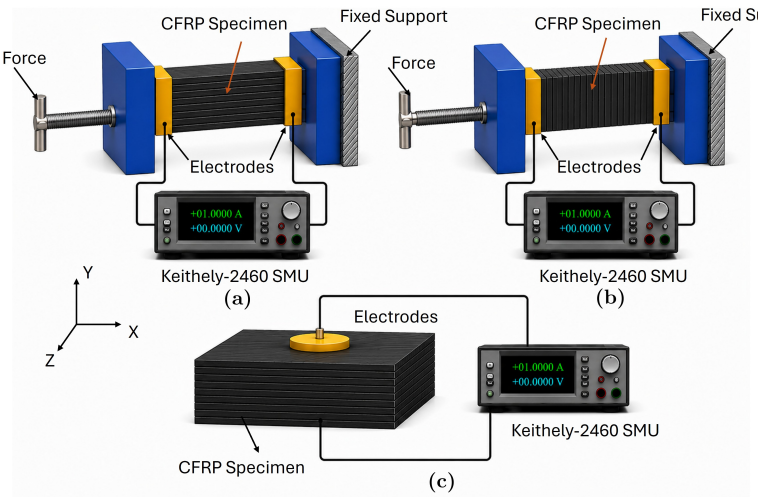


Figure A1. Schematic showing electrical conductivity measurement of composite coupons (**a**) along the fiber direction σ_x (**b**) transverse to the fiber direction σ_y and (**c**) through-thickness direction σ_z.

Appendix A.5. EMI Shielding Effectiveness: Vector Network Analyser (VNA) and Waveguide

Figure 7 schematically shows the experimental setup used to record the EMI shielding effectiveness of composite coupons using Vector Network Analyzer (N5230, Keysight Technologies, Santa Rosa, CA, USA) and a rectangular waveguide (WR-90, Keysight, USA). Before measurements, the VNA is calibrated using a standard calibration kit (X11644A) to ensure accurate and reliable data. (Figure A2a,b). The sample dimensions are 22.86 $\times$ 10.16 $\times$ 2 mm^3. The EMI shielding effectiveness of samples is measured in two configurations. While carbon fibers are aligned in the direction of the electric field (Figure A2c) in the first configuration, they are aligned perpendicular to it (Figure A2d) in the second configuration. Again, anisotropy of the material causes the shielding characteristics to be different in the two cases.

VNA measures the reflection and transmission coefficients when the sample is exposed to electromagnetic waves. S_{21} is transmission coefficients of EM waves from port-1 to port-2 whereas S_{11} and S_{22} are the reflection coefficients. Shielding effectiveness is calculated from the S-parameters using the following relations,

$$\mathrm{SE}_R = 10\log_{10}\left|\frac{1}{1-|S_{11}|^2}\right| \tag{A5}$$

$$\mathrm{SE}_A = 10\log_{10}\left|\frac{1-|S_{11}|^2}{|S_{21}|^2}\right| \tag{A6}$$

$$\mathrm{SE}_T = \mathrm{SE}_R + \mathrm{SE}_A \tag{A7}$$

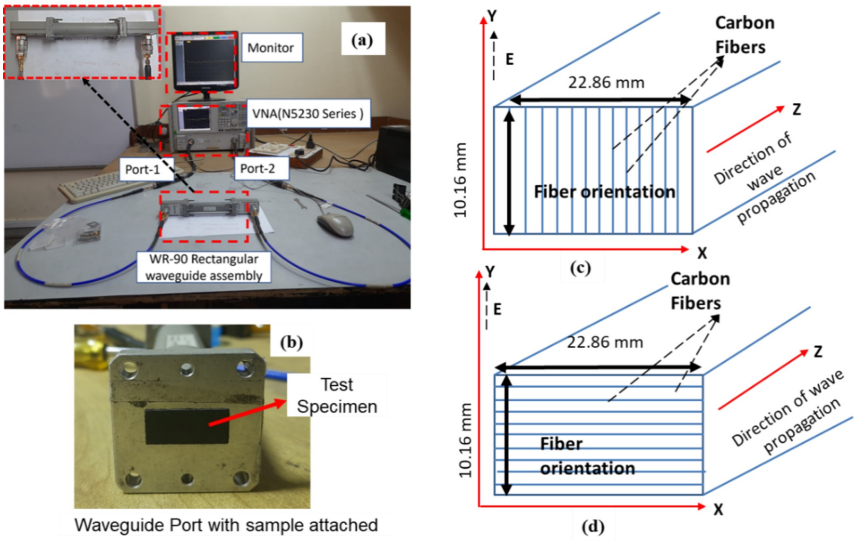


Figure A2. (**a**) VNA and (**b**) rectangular waveguide used to measure the EMI shielding of composite coupons. Orientation of carbon fibers (**c**) along and (**b**) perpendicular to the applied field during EMI measurements.

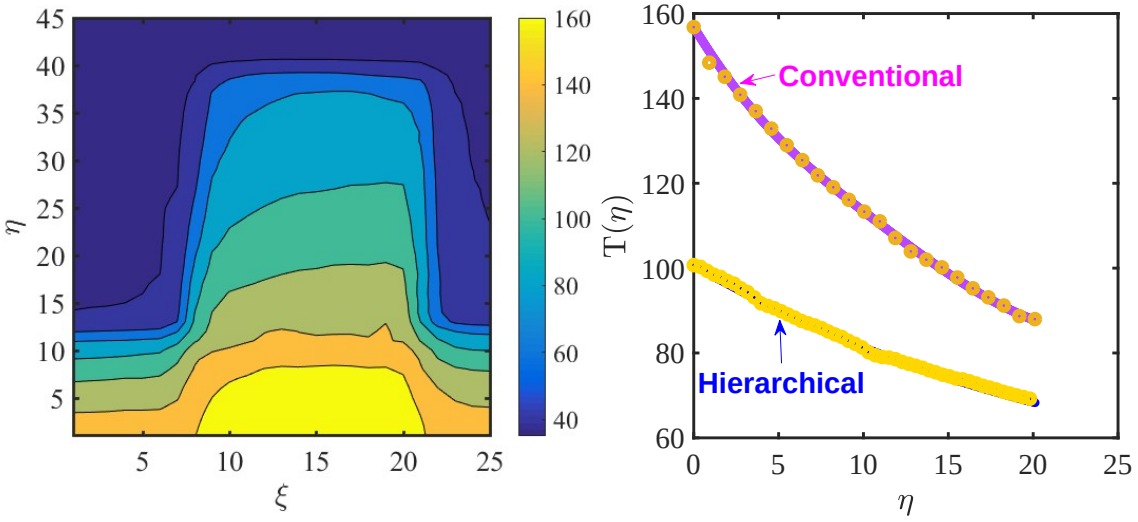
Appendix A.6. Thermal Conductivity: Fin Equations and Laser Flash Analyser

Appendix A.6.1. In-Plane Thermal Conductivity

The in-plane thermal conductivities along (k_x) and perpendicular (k_y) to the fiber direction are measured using the equations of a thermal fin. At steady state, the temperature in the fin (see Figure A3a) is effectively one dimensional, with negligible variation in the ξ direction. The variation of $T(\eta)$ for a typical case is shown in Figure A3c. The temperature distribution is governed by the simple equation of the fin

$$\frac{d^2\theta}{d\eta^2} - \frac{hP}{Ak_\eta}\theta = 0 \tag{A8}$$

here $\theta = T - T_\infty$, with $T(\eta = 0) = T_0$, the constant temperature of the base. Further, h, A and P are the convective heat transfer coefficient, transverse area, and perimeter of the fin respectively. When the fin is mounted such that the fibers are directed along η, $k_\eta = k_x$. Similarly, when fibers are along ξ, $k_\eta = k_y$. The thermal conductivities are determined by adjusting k_η such that the experimentally observed temperature variation matches with that obtained from Equation (A8) (see Figure A3b).



(a) **(b)**

Figure A3. (**a**) Contours of temperature $T(\eta, \xi)$ on the surface of a typical fin sample and (**b**) variation of temperature along the length of the specimen at a fixed ξ for CF/ep and CNTGCF/ep laminates. The curves fitted using the fin equation are shown with dotted lines.

Steady-state temperature profiles of samples mounted on a hot plate in a rectangular fin configuration are used to compute the in-plane conductivities. The composite samples (length 60 mm and width 20 mm) along with a reference sample (Aluminum, see Figure A4) are fixed on a hot plate with thermally conducting epoxy adhesive. The hot plate is set at a constant temperature and the temperatures of the hot plate, sample, and surroundings are measured with thermocouples. Additionally, at the steady state, 2-dimensional temperature profiles on the surface of the samples are recorded with an Infrared camera (FLIR A310; Teledyne FLIR LLC, Wilsonville, OR, USA) to deduce k_x and k_y.

Appendix A.6.2. Through Thickness Thermal Conductivity

We use a laser flash analyser (NanoFlash LFA 447, NETZSCH-Gerätebau GmbH, Selb, Germany) to measure the through thickness thermal conductivity. Determination of k_x and k_y is somewhat more challenging.

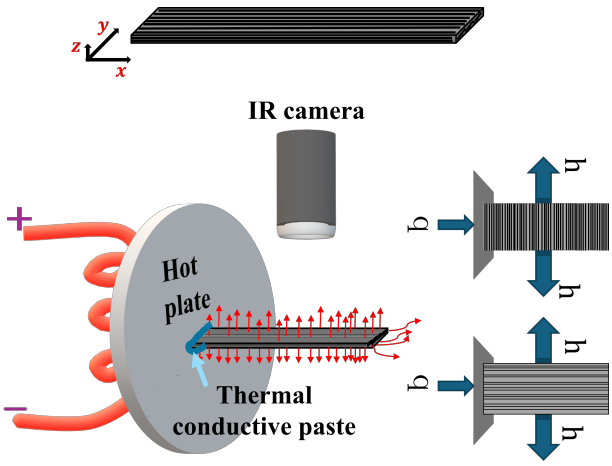


Figure A4. Hot plate vertical fin set up used to obtain the in-plane thermal conductivities (k_x and k_y) of conventional and hierarchical composite samples.

References

1. Zhang, J.; Lin, G.; Vaidya, U.; et al. Past, present and future prospective of global carbon fibre composite developments and applications. *Compos. Part B Eng.* **2023**, *250*, 110463. https://doi.org/10.1016/j.compositesb.2022.110463.
2. Kizaki, T.; Zhang, J.; Yao, Q.; et al. Continuous manufacturing of CFRP sheets by rolling for rapid fabrication of long CFRP products. *Compos. Part B Eng.* **2020**, *189*, 107896. https://doi.org/10.1016/j.compositesb.2020.107896.
3. Achim, V.; Ruiz, E. Guiding selection for reduced process development time in RTM. *Int. J. Mater. Form.* **2010**, *3*(Suppl. 2), 1277–1286. https://doi.org/10.1007/s12289-009-0630-6.
4. Sahu, R.; Ponnusami, S.A.; Weimer, C.; et al. Interface engineering of carbon fiber composites using CNT: A review. *Polym. Compos.* **2024**, *45*, 9–42. https://doi.org/10.1002/pc.27772.
5. Zhao, Z.; Teng, K.; Li, N.; et al. Mechanical, thermal and interfacial performances of carbon fiber reinforced composites flavored by carbon nanotube in matrix/interface. *Compos. Struct.* **2017**, *159*, 761–772. https://doi.org/10.1016/j.compstruct.2016.10.022.
6. Pozegic, T.R.; Anguita, J.V.; Hamerton, I.; et al. Multi-Functional Carbon Fibre Composites using Carbon Nanotubes as an Alternative to Polymer Sizing. *Sci. Rep.* **2016**, *6*, 37334. https://doi.org/10.1038/srep37334.
7. Kandare, E.; Khatibi, A.A.; Yoo, S.; et al. Improving the through-thickness thermal and electrical conductivity of carbon fibre/epoxy laminates by exploiting synergy between graphene and silver nano-inclusions. *Compos. Part A Appl. Sci. Manuf.* **2015**, *69*, 72–82. https://doi.org/10.1016/j.compositesa.2014.10.024.
8. Hao, M.; Qian, X.; Zhang, Y.; et al. Thermal conductivity enhancement of carbon fiber/epoxy composites via constructing three-dimensionally aligned hybrid thermal conductive structures on fiber surfaces. *Compos. Sci. Technol.* **2023**, *231*, 109800. https://doi.org/10.1016/j.compscitech.2022.109800.
9. Sung, D.H.; Kim, M.; Park, Y.B. Prediction of thermal conductivities of carbon-containing fiber-reinforced and multiscale hybrid composites. *Compos. Part B Eng.* **2018**, *133*, 232–239. https://doi.org/10.1016/j.compositesb.2017.09.032.
10. Qian, H.; Bismarck, A.; Greenhalgh, E.S.; et al. Hierarchical Composites Reinforced with Carbon Nanotube Grafted Fibers: The Potential Assessed at the Single Fiber Level. *Chem. Mater.* **2008**, *20*, 1862–1869. https://doi.org/10.1021/cm702782j.
11. Qian, H.; Greenhalgh, E.S.; Shaffer, M.S.P.; et al. Carbon nanotube-based hierarchical composites: A review. *J. Mater. Chem.* **2010**, *20*, 4751–4762. https://doi.org/10.1039/c000041h.
12. Downs, W.B.; Baker, R.T.K. Novel carbon fiber-carbon filament structures. *Carbon* **1991**, *29*, 1173–1179. https://doi.org/10.1016/0008-6223(91)90035-h.
13. Downs, W.B.; Baker, R.T.K. Modification of the surface properties of carbon fibers via the catalytic growth of carbon nanofibers. *J. Mater. Res.* **1995**, *10*, 625–633. https://doi.org/10.1557/jmr.1995.0625.
14. Thostenson, E.T.; Li, W.Z.; Wang, D.Z.; et al. Carbon nanotube/carbon fiber hybrid multiscale composites. *J. Appl. Phys.* **2002**, *91*, 6034–6037. https://doi.org/10.1063/1.1466880.
15. Ou, Y.; Wu, L.; Mao, D. Hierarchical mode I interlaminar toughening of unidirectional CFRP laminates by the synergistic effects of CNT powders and veils. *Compos. Part A Appl. Sci. Manuf.* **2023**, *168*, 107464. https://doi.org/10.1016/j.compositesa.2023.107464.
16. Reynaud, E.; Gauthier, C.; Perez, J. Nanophases in polymers. *Rev. Métall.* **1999**, *96*, 169–176. https://doi.org/10.1051/metal/199996020169.
17. Winey, K.I.; Vaia, R.A. Polymer Nanocomposites. *MRS Bull.* **2007**, *32*, 314–322. https://doi.org/10.1557/mrs2007.229.
18. Pandey, J.C.; Gupta, N. Estimation of interphase thickness of epoxy-based nanocomposites. *IEEE Trans. Dielectr. Electr. Insul.* **2016**, *23*, 2747–2756. https://doi.org/10.1109/tdei.2016.7736834.
19. Yuan, X.; Zhu, B.; Cai, X.; et al. Nanoscale toughening of carbon fiber-reinforced epoxy composites through different surface

treatments. *Polym. Eng. Sci.* **2019**, *59*, 625–632. https://doi.org/10.1002/pen.24978.

20. Gojny, F.; Wichmann, M.; Fiedler, B.; et al. Influence of different carbon nanotubes on the mechanical properties of epoxy matrix composites—A comparative study. *Compos. Sci. Technol.* **2005**, *65*, 2300–2313. https://doi.org/10.1016/j.compscitech.2005.04.021.
21. Hernández-Pérez, A.; Avilés, F.; May-Pat, A.; et al. Effective properties of multiwalled carbon nanotube/epoxy composites using two different tubes. *Compos. Sci. Technol.* **2008**, *68*, 1422–1431. https://doi.org/10.1016/j.compscitech.2007.11.001.
22. Tang, L.C.; Zhang, H.; Han, J.H.; et al. Fracture mechanisms of epoxy filled with ozone functionalized multi-wall carbon nanotubes. *Compos. Sci. Technol.* **2011**, *72*, 7–13. https://doi.org/10.1016/j.compscitech.2011.07.016.
23. Gupta, H.; Srivastava, M.; Agnihotri, P.K.; et al. A Critical Assessment of Electrical Conductivity and Multifunctionality of MWCNT/Epoxy Nanocomposites. *IEEE Trans. Dielectr. Electr. Insul.* **2025**, *32*, 1324–1332. https://doi.org/10.1109/tdei.2025.3562536.
24. Steiner, S.A.; Li, R.; Wardle, B.L. Circumventing the Mechanochemical Origins of Strength Loss in the Synthesis of Hierarchical Carbon Fibers. *ACS Appl. Mater. Interfaces* **2013**, *5*, 4892–4903. https://doi.org/10.1021/am4006385.
25. Gangineni, P.K.; Yandrapu, S.; Ghosh, S.K.; et al. Mechanical behavior of graphene decorated carbon fiber reinforced polymer composites: An assessment of the influence of functional groups. *Compos. Part A Appl. Sci. Manuf.* **2019**, *122*, 36–44. https://doi.org/10.1016/j.compositesa.2019.04.017.
26. He, P.; Huang, B.; Liu, L.; et al. Preparation of multiscale graphene oxide-carbon fabric and its effect on mechanical properties of hierarchical epoxy resin composite. *Polym. Compos.* **2016**, *37*, 1515–1522. https://doi.org/10.1002/pc.23321.
27. Jiang, J.; Yao, X.; Xu, C.; et al. Influence of electrochemical oxidation of carbon fiber on the mechanical properties of carbon fiber/graphene oxide/epoxy composites. *Compos. Part A Appl. Sci. Manuf.* **2017**, *95*, 248–256. https://doi.org/10.1016/j.compositesa.2017.02.004.
28. Deng, C.; Jiang, J.; Liu, F.; et al. Influence of surface properties of graphene oxide/carbon fiber hybrid fiber by oxidative treatments combined with electrophoretic deposition. *Surf. Interface Anal.* **2016**, *48*, 212–217. https://doi.org/10.1002/sia.5944.
29. Gong, S.; Zhu, Z.H.; Arjmand, M.; et al. Effect of carbon nanotubes on electromagnetic interference shielding of carbon fiber reinforced polymer composites. *Polym. Compos.* **2018**, *39*, E655–E663. https://doi.org/10.1002/pc.24084.
30. Davis, D.C.; Wilkerson, J.W.; Zhu, J.; et al. Improvements in mechanical properties of a carbon fiber epoxy composite using nanotube science and technology. *Compos. Struct.* **2010**, *92*, 2653–2662. https://doi.org/10.1016/j.compstruct.2010.03.019.
31. Zhang, Q.; Liu, J.; Sager, R.; et al. Hierarchical composites of carbon nanotubes on carbon fiber: Influence of growth condition on fiber tensile properties. *Compos. Sci. Technol.* **2009**, *69*, 594–601. https://doi.org/10.1016/j.compscitech.2008.12.002.
32. De Greef, N.; Zhang, L.; Magrez, A.; et al. Direct growth of carbon nanotubes on carbon fibers: Effect of the CVD parameters on the degradation of mechanical properties of carbon fibers. *Diam. Relat. Mater.* **2015**, *51*, 39–48. https://doi.org/10.1016/j.diamond.2014.11.002.
33. Zhang, W.; Deng, X.; Sui, G.; et al. Improving interfacial and mechanical properties of carbon nanotube-sized carbon fiber/epoxy composites. *Carbon* **2019**, *145*, 629–639. https://doi.org/10.1016/j.carbon.2019.01.063.
34. Agnihotri, P.K.; Basu, S.; Kar, K.K. Effect of carbon nanotube length and density on the properties of carbon nanotube-coated carbon fiber/polyester composites. *Carbon* **2011**, *49*, 3098–3106. https://doi.org/10.1016/j.carbon.2011.03.032.
35. Yesu, A.; Srivastava, M.; Agnihotri, P.K.; et al. Minimizing environmental degradation in fracture toughness of carbon fiber/epoxy composites using carbon nanotubes. *Eng. Fract. Mech.* **2023**, *294*, 109734. https://doi.org/10.1016/j.engfracmech.2023.109734.
36. Khan, S.; Bedi, H.S.; Agnihotri, P.K. Augmenting mode-II fracture toughness of carbon fiber/epoxy composites through carbon nanotube grafting. *Eng. Fract. Mech.* **2018**, *204*, 211–220. https://doi.org/10.1016/j.engfracmech.2018.10.014.
37. Bedi, H.S.; Billing, B.K.; Agnihotri, P.K. Interfacial shear strength of carbon nanotubes based hybrid composites: Effect of loading rate. *Frat. Integrità Strutt.* **2019**, *13*, 571–576. https://doi.org/10.3221/igf-esis.48.55.
38. Bedi, H.S.; Padhee, S.S.; Agnihotri, P.K. Effect of carbon nanotube grafting on the wettability and average mechanical properties of carbon fiber/polymer multiscale composites. *Polym. Compos.* **2018**, *39*, E1184–E1195. https://doi.org/10.1002/pc.24714.
39. Bedi, H.S.; Tiwari, M.; Agnihotri, P.K. Quantitative determination of size and properties of interphases in carbon nanotube-based multiscale composites. *Carbon* **2018**, *132*, 181–190. https://doi.org/10.1016/j.carbon.2018.02.059.
40. Kar, K.K.; Kumar, P.; Iyengar, N.G.R.; et al. Carbon Nanotube and Nanoparticles Coated Carbon Fiber Reinforced Polymer Hybrid Composite with Improved Thermomechanical Properties and a Process for Preparation Thereof. Patent No. 1813/DEL/2005, 14 July 2005.
41. Bedi, H.S.; Billing, B.K.; Agnihotri, P.K. Interphase engineering in carbon fiber/epoxy composites: Rate sensitivity of interfacial shear strength and interfacial fracture toughness. *Polym. Compos.* **2020**, *41*, 2803–2815. https://doi.org/10.1002/pc.25577.
42. Qian, H.; Bismarck, A.; Greenhalgh, E.S.; et al. Carbon nanotube grafted carbon fibres: A study of wetting and fibre fragmentation. *Compos. Part A Appl. Sci. Manuf.* **2010**, *41*, 1107–1114. https://doi.org/10.1016/j.compositesa.2010.04.004.
43. Chatterjee, K.; Kumar, V.; Agnihotri, P.K.; et al. On the Importance of the Metal Catalyst Layer to the Performance of CNT-Based Supercapacitor Electrodes. *IEEE Trans. Nanotechnol.* **2025**, *24*, 48–53. https://doi.org/10.1109/tnano.2024.3523412.
44. Qin, J.; Wang, C.; Yao, Z.; et al. Growing carbon nanotubes on continuous carbon fibers to produce composites with

improved interfacial properties: A step towards commercial production and application. *Compos. Sci. Technol.* **2021**, *211*, 108870. https://doi.org/10.1016/j.compscitech.2021.108870.

45. Lv, P.; Feng, Y.Y.; Zhang, P.; et al. Increasing the interfacial strength in carbon fiber/epoxy composites by controlling the orientation and length of carbon nanotubes grown on the fibers. *Carbon* **2011**, *49*, 4665–4673. https://doi.org/10.1016/j.carbon.2011.06.064.
46. Zheng, L.; Wang, Y.; Qin, J.; et al. Scalable manufacturing of carbon nanotubes on continuous carbon fibers surface from chemical vapor deposition. *Vacuum* **2018**, *152*, 84–90. https://doi.org/10.1016/j.vacuum.2018.03.011.
47. Deng, Y.; Islam, M.S.; Tong, L. Effects of grafting strength and density on interfacial shear strength of carbon nanotube grafted carbon fibre reinforced composites. *Compos. Sci. Technol.* **2018**, *168*, 195–202. https://doi.org/10.1016/j.compscitech.2018.09.025.
48. Gao, B.; Zhang, R.; He, M.; et al. Effect of a multiscale reinforcement by carbon fiber surface treatment with graphene oxide/carbon nanotubes on the mechanical properties of reinforced carbon/carbon composites. *Compos. Part A Appl. Sci. Manuf.* **2016**, *90*, 433–440. https://doi.org/10.1016/j.compositesa.2016.08.012.
49. Li, R.; Lachman, N.; Florin, P.; et al. Hierarchical carbon nanotube carbon fiber unidirectional composites with preserved tensile and interfacial properties. *Compos. Sci. Technol.* **2015**, *117*, 139–145. https://doi.org/10.1016/j.compscitech.2015.04.014.
50. Agnihotri, P.K.; Kar, K.K.; Basu, S. Cohesive zone model of carbon nanotube-coated carbon fiber/polyester composites. *Model. Simul. Mater. Sci. Eng.* **2012**, *20*, 035014. https://doi.org/10.1088/0965-0393/20/3/035014.
51. Zhao, Z.J.; Zhang, B.Y.; Du, Y.; et al. MWCNT modified structure-conductive composite and its electromagnetic shielding behavior. *Compos. Part B Eng.* **2017**, *130*, 21–27. https://doi.org/10.1016/j.compositesb.2017.07.033.
52. Xiao, C.; Tan, Y.; Wang, X.; et al. Study on interfacial and mechanical improvement of carbon fiber/epoxy composites by depositing multi-walled carbon nanotubes on fibers. *Chem. Phys. Lett.* **2018**, *703*, 8–16. https://doi.org/10.1016/j.cplett.2018.05.012.
53. Xu, N.; Li, Y.; Zheng, T.; et al. A mussel-inspired strategy for CNT/carbon fiber reinforced epoxy composite by hierarchical surface modification. *Colloids Surf. A Physicochem. Eng. Asp.* **2022**, *635*, 128085. https://doi.org/10.1016/j.colsurfa.2021.128085.
54. Yao, Z.; Wang, C.; Lu, R.; et al. Fracture investigation of functionalized carbon nanotubes-grown carbon fiber fabrics/epoxy composites. *Compos. Sci. Technol.* **2020**, *195*, 108161. https://doi.org/10.1016/j.compscitech.2020.108161.
55. Singh, B.P.; Choudhary, V.; Saini, P.; et al. Designing of epoxy composites reinforced with carbon nanotubes grown carbon fiber fabric for improved electromagnetic interference shielding. *AIP Adv.* **2012**, *2*, 022151. https://doi.org/10.1063/1.4730043.
56. Du, H.; He, Y.; Song, H.; et al. Real-Time Structural Monitoring and Effective Interlaminar Reinforcement of Carbon Fiber Composites Hybrid with Surface Modified Non-Woven Silk Fabric. *Polym. Compos.* **2025**, *46*, 14943–14956. https://doi.org/10.1002/pc.30104.
57. Zhang, C.; Zhang, G.; Shi, X.; et al. Effects of carbon nanotubes on the interlaminar shear strength and fracture toughness of carbon fiber composite laminates: A review. *J. Mater. Sci.* **2022**, *57*, 2388–2410. https://doi.org/10.1007/s10853-021-06734-z.
58. Song, Y.; Zheng, N.; Dong, X.; et al. Flexible Carboxylated CNT/PA66 Nanofibrous Mat Interleaved Carbon Fiber/Epoxy Laminates with Improved Interlaminar Fracture Toughness and Flexural Properties. *Ind. Eng. Chem. Res.* **2020**, *59*, 1151–1158. https://doi.org/10.1021/acs.iecr.9b05854.
59. Gupta, H.; Agnihotri, P.K.; Basu, S.; et al. Carbon nanotube grafting for better electromagnetic shielding with carbon fiber/epoxy composites. *Polym. Compos.* **2025**, *46*, S856–S866. https://doi.org/10.1002/pc.30003.
60. Badakhsh, A.; An, K.H.; Kim, B.J. Enhanced Surface Energetics of CNT-Grafted Carbon Fibers for Superior Electrical and Mechanical Properties in CFRPs. *Polymers* **2020**, *12*, 1432. https://doi.org/10.3390/polym12061432.
61. Lee, G.; Sung, M.; Youk, J.H.; et al. Improved tensile strength of carbon nanotube-grafted carbon fiber reinforced composites. *Compos. Struct.* **2019**, *220*, 580–591. https://doi.org/10.1016/j.compstruct.2019.04.037.
62. Srivastava, M.K.; Gupta, H.; Gupta, N.; et al. Electromagnetic Shielding WithCFRPComposites: Conducting Matrix Versus Conducting Fibers. *Polym. Compos.* **2025**, *46*, 17029–17040. https://doi.org/10.1002/pc.70093.
63. Chauhan, A.; Agnihotri, P.K.; Basu, S. Molecular dynamic study on modulating the interfacial thermal conductivity of carbon fiber/epoxy interfaces. *Comput. Mater. Sci.* **2023**, *217*, 111914. https://doi.org/10.1016/j.commatsci.2022.111914.
64. Chen, J.; Xiong, X.; Xiao, P. The effect of carbon nanotube growing on carbon fibers on the microstructure of the pyrolytic carbon and the thermal conductivity of carbon/carbon composites. *Mater. Chem. Phys.* **2009**, *116*, 57–61. https://doi.org/10.1016/j.matchemphys.2009.02.044.
65. Su, S.; Wang, Y.; Qin, J.; et al. Continuous method for grafting CNTs on the surface of carbon fibers based on cobalt catalyst assisted by thiourea. *J. Mater. Sci.* **2019**, *54*, 12498–12508. https://doi.org/10.1007/s10853-019-03827-8.
66. Anthony, D.B.; Sui, X.; Kellersztein, I.; et al. Continuous carbon nanotube synthesis on charged carbon fibers. *Compos. Part A Appl. Sci. Manuf.* **2018**, *112*, 525–538. https://doi.org/10.1016/j.compositesa.2018.05.027.
67. Larsson, C.; Larsson, F.; Tavano, R.; et al. Poro-mechanical analysis of a structural battery electrolyte: Experimental study and model calibration. *Mech. Mater.* **2026**, *216*, 105632. https://doi.org/10.1016/j.mechmat.2026.105632.
68. Chaudhary, R.; Tavano, R.; Xu, J.; et al. Lithium-Ion Transport in Carbon Fibers for Structural Batteries. *Adv. Energy Sustain. Res.* **2026**, *7*, e202500377. https://doi.org/10.1002/aesr.202500377.